An Improved Vector Fitting Approach for Obtaining the Novel Impulse Response for a Diffraction on a Dielectric Convex Obstacle

Piotr Górniak
Poznań University of Technology
Department of Electronics and Telecommunications
Poznań, Poland
pgorniak@et.put.poznan.pl

Wojciech Bandurski
Poznań University of Technology
Department of Electronics and Telecommunications
Poznań, Poland
wojciech.bandurski@put.poznan.pl

***Abstract*—In the paper we present the improved VF (Vector Fitting) approach for the derivation of a closed form impulse response of a diffraction ray that creeps two dimensional (2D) dielectric convex obstacle in the form of 2D cylinder. The impulse response is obtained by applying a rational function approximation of the transfer function of a creeping ray. The transfer function is formulated according to UTD (Uniform Theory of Diffraction) dedicated for a dielectric convex object. Then the inverse Laplace transform is applied. The impulse response has a simple form. It is a sum of exponential functions which can be in a very effective way applied to simulations of UWB signal propagation in channels containing convex obstacles.**

***Index Terms*—creeping ray, UTD – Uniform Theory of Diffraction, UWB – Ultra-Wide-Band, time-domain.**

I. INTRODUCTION

UWB technology enables many beneficial features in transmission and radar area. In order to take the advantage of these features careful UWB system analysis are performed. The important component of an UWB system is a propagation channel. Due to a very wide range of UWB signal spectrum the models (functions) of channel components (obstacles) have to be derived for the purpose of proper UWB channel investigation. The natural choice of the domain for UWB propagation analysis is the time-domain, and the usage of impulse responses. These can be found in an empirical way with the usage of measurement results or through simulations. The paper deals with the latter one for the case of UWB channels that comprise obstacles (e.g. people) which can be modeled by convex objects (cylinders in 3D case or arcs in 2D case). In [1] we presented the way for obtaining the closed form novel impulse response of a diffraction ray for a good convex conductor case. Although such an object can be a good model of a human body in a wireless channel [2] the physical parameters of this object do not match those of human body. A better choice for modeling a human body is to use a dielectric object. Our aim is to present the procedure for obtaining the closed form impulse response of an UTD creeping ray for a dielectric object case. The impulse response, which we present, has a form that enables effective (fast and accurate) simulations of UWB signal diffraction on dielectric convex obstacles. We verify the derived impulse response through simulations of an UWB pulse diffraction on a convex dielectric 2D cylinder. As a reference we use the results obtained by IFFT applied to a creeping ray transfer function. The paper is organized as follows. In Section 2 we describe the dielectric convex obstacle model. Section 3 is devoted to the derivation of the new impulse response for a dielectric convex object. In Section 4 the results of the verification of the new approach are presented. We make conclusions in Section 5

II. DIELECTRIC CONVEX OBSTACLE MODEL

The scenario of a diffraction ray creeping on a 2D dielectric convex object is shown in Fig. 1.

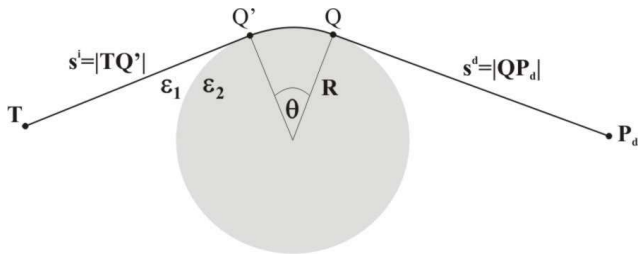

Fig. 1. The UTD ray creeping on a dielectric 2D cylinder.

The main parameters of the scenario are: θ – angular creeping distance, R – radius of an object, s^i – the distance from the field source point – T to the attachment point – Q' and s^d – the distance from the shedding point – Q to the observation point – P_d. The cylinder has a permittivity equal to ε_2 while the surrounding medium permittivity is ε_1. The UTD amplitude term of transfer function of the ray is given by [1]:

$$H_{AD}(\omega) = H_{A1}(\omega) + H_{A2}(\omega), \tag{1}$$

where

$$H_{A1}(\omega) = \sqrt{\frac{\nu}{2\pi\omega\theta^2}} \cdot e^{-j\frac{\pi}{4}} F(X_d), \tag{2}$$

$$H_{A2D}(\omega) = -\left(\frac{2vR^2}{\omega}\right)^{1/6} e^{-j\frac{\pi}{4}} \begin{cases} p_D(\xi_d) \\ q_D(\xi_d) \end{cases}. \quad (3)$$

The function $F(X_d)$ is described in e.g. [3]. The $p_D(\xi_d)$ and $q_D(\xi_d)$ are the Fock scattering functions for the soft and the hard polarization case respectively. The subscript D indicates that we use their forms dedicated for dielectric objects. For the hard polarization case and $\varepsilon_1 = \varepsilon_0$ this function is given by [4]:

$$q_D(\xi_d, \varepsilon_r) = \frac{e^{-j\pi/4}}{\sqrt{\pi}} \int_{-\infty}^{\infty} \frac{V'(\tau) - u(\varepsilon_r, \tau)V(\tau)}{w_2'(\tau) - u(\varepsilon_r, \tau)w_2(\tau)} e^{j\xi_d \tau} d\tau \quad (4)$$

where:

$$u(\varepsilon_r, \tau) = M \frac{H_v^{(2)'}\left(\sqrt{\varepsilon_r}\beta_0 R\right)}{H_v^{(2)}\left(\sqrt{\varepsilon_r}\beta_0 R\right)} \frac{1}{\sqrt{\varepsilon_r}}, \quad v = \beta_0 R + M\tau \quad (5)$$

$$M = \left(\frac{\beta_0 R}{2}\right)^{1/3}, \ \beta_0 = \frac{\omega}{c}, \quad \xi_d = M \cdot \theta \quad (6)$$

where ε_r is a relative permittivity of a dielectric object and c is the speed of light.

III. Derivation of the New Impulse Response

In [1] we presented the novel closed form impulse response of a creeping ray for the case of a good conducting object. We introduced the new variable ξ_{dsub} (proportional to ω) in order to present (7) as the product of this new variable function and the function independent of ω:

$$H_{A2}(\omega) = -\sqrt{R\theta} \cdot e^{-j\frac{\pi}{4}} \frac{\begin{cases} p\left(\xi_{dsub}^{1/3}\right) \\ q\left(\xi_{dsub}^{1/3}\right) \end{cases}}{\sqrt{\xi_{dsub}^{1/3}}}. \quad (7)$$

Then the VF approximation were performed in the established ξ_{dsub} limits and the inverse Laplace transformation were applied. In order to find an impulse response of a creeping ray for a dielectric object case the algorithm from [1] have to be improved.

First, in order to have the whole impulse response in the form of the sum of exponential functions, we choose the variable for approximation of (2). This variable is $X_{dsub} = X_d$ and is equal $\beta_0 L_d \theta^2/2$, where $L_d = s^i \cdot s^d / (s^i + s^d)$. Then (2) can be rearranged to (8), which we approximate with VF to the form in (9). The limits of X_{dsub} values, for which the approximation is performed, are chosen as the limits of ξ_{dsub} in [1]. The range of considered values of radius of a convex object can be set e.g. to $R \in \langle 0.2, 1\rangle$m. The lower limit value is the minimum value of a cylinder radius that is used in literature to model a human body. The upper limit value is reserved for other convex obstacles that can occur in an UWB channel. The lower and upper limit of θ value can be established to $3 \cdot 10^{-4}$ rad and π rad respectively. The first value in chosen in the way that its substitution in $H_{A1}(\omega)$ instead of 0 does not cause the relative deviation from an accurate result above 0.1%. The second value of θ parameter can occur when sensor applications are taken into consideration (the wave creeps an object and goes back towards the transmitter). The range of separation coefficient value can be set e.g. to $L_d \in \langle 0.5, 4\rangle$m for the cases of smaller and bigger separation of an obstacle and antennas. The lower and upper limit values of ω depend on the spectra of UWB pulses that are in our concern. We can assume that the spectra of pulses will be in the range <0.1, 10>GHz. Then the range of pulsation values is $\omega \in \langle 2\pi \cdot 10^8, 2\pi \cdot 10^{10}\rangle$rad/s. For the above limits of the scenario parameters, the range of the approximation domain for (8) in logarithmic scale is $X_{dsub} \in \langle 10^{-8}, 10^3\rangle$.

$$H_{A1}(\omega) = \sqrt{\frac{L_d}{4\pi}} \cdot e^{-j\frac{\pi}{4}} \frac{F(X_{dsub})}{\sqrt{X_{dsub}}}. \quad (8)$$

$$H_{A1}(\omega) \approx \sqrt{\frac{L_d}{4\pi}} \cdot \sum_{j=1}^{J} \frac{C_{1j} \cdot 2c / L_d \theta^2}{j\omega + A_{1j} \cdot 2c / L_d \theta^2}. \quad (9)$$

The second component of (1) cannot be rearranged to the product of a function dependent only from the variable similar to ξ_{dsub} and a function independent from ω. Therefore the procedure from [1] have to be improved in order to derive the new time-domain equivalent of (3).

First, we rearrange (4) by substituting the new variable $M_{sub} = M^3$ as fallows.

$$q_D(M, \theta, \varepsilon_r) = \frac{e^{-j\pi/4}}{\sqrt{\pi}} \int_{-\infty}^{\infty} \frac{V'(\tau) - u(\varepsilon_r, \tau)V(\tau)}{w_2'(\tau) - u(\varepsilon_r, \tau)w_2(\tau)} e^{j(M_{sub})^{1/3}\theta \cdot \tau} d\tau \quad (10)$$

Then using (5) and the results from [5] we can rearrange the function that will be approximated to following form.

$$H_{sub}(\omega) = \frac{e^{-j\frac{\pi}{4}}}{\sqrt{\pi}} \frac{\left(C_1(M_{sub}, \theta, \varepsilon_r) + C_2(M_{sub}, \theta, \varepsilon_r)\right)}{\sqrt{M_{sub}^{1/3}\theta}} \quad (11a)$$

$$C_1(M_{sub}, \theta, \varepsilon_r) = \frac{e^{-j\frac{\pi}{6}}}{2} \times \int_0^{\infty} \frac{e^{-j\frac{\pi}{6}} Ai'(\tau) - u\left(M_{sub}, \varepsilon_r, \tau \cdot e^{-j\frac{2\pi}{3}}\right) e^{j\frac{\pi}{6}} Ai(\tau)}{e^{j\frac{\pi}{6}} Ai'\left(\tau \cdot e^{j\frac{2\pi}{3}}\right) - u\left(M_{sub}, \varepsilon_r, \tau \cdot e^{-j\frac{2\pi}{3}}\right) e^{-j\frac{\pi}{6}} Ai\left(\tau \cdot e^{j\frac{2\pi}{3}}\right)} \times e^{-j\sqrt[3]{M_{sub}}\theta \cdot \tau \cdot e^{-j\frac{2\pi}{3}}} d\tau \quad (11b)$$

$$C_2(M_{sub}, \theta, \varepsilon_r) = -\frac{1}{2} \times \int_0^{\infty} \frac{Ai'(\tau) + u(M_{sub}, \varepsilon_r, \tau) Ai(\tau)}{e^{j\frac{\pi}{6}} Ai'\left(\tau \cdot e^{-j\frac{2\pi}{3}}\right) - u\left(M_{sub}, \varepsilon_r, \tau \cdot e^{-j\frac{2\pi}{3}}\right) e^{-j\frac{\pi}{6}} Ai\left(\tau \cdot e^{-j\frac{2\pi}{3}}\right)} \times e^{-j\sqrt[3]{M_{sub}}\theta \cdot \tau} d\tau \quad (11c)$$

$$u(M_{sub}, \varepsilon_r t) = M_{sub}^{1/3} \frac{H_v^{(2)'}\left(2\sqrt{\varepsilon_r} M_{sub}\right)}{H_v^{(2)}\left(2\sqrt{\varepsilon_r} M_{sub}\right)} \frac{1}{\sqrt{\varepsilon_r}}, \quad v = 2M_{sub} + M_{sub}^{1/3} t \quad (11d)$$

For the sufficient accuracy of the results of calculations of (10) the upper limits of the integrals from (11) can be set to 20. We see now that (11a) depends on 3 variables. For given values of the parameters θ and ε_r the process of approximation of (12) in the M_{sub} domain can be conducted.

$$H_{A2D}(\omega) = -\sqrt{R\theta}\cdot e^{-j\frac{\pi}{4}}\frac{q_d(M_{dsub},\theta,\varepsilon_r)}{\sqrt{M_{dsub}^{1/3}\cdot\theta}}. \quad (12)$$

The limits of M_{sub} values are set as in X_{dsub} and ξ_{dsub} cases. For the limits of parameters values presented previously the range of the new variable in logarithmic scale is $M_{sub} \in <10^{-1}, 10^{2}>$. Now the aim is to make the values of residues and poles, resulting from VF approximations, the functions of θ and ε_r. We make it by introducing the new variable Z_{sub}, which is the function of θ and ε_r. The description of the procedure which we use for obtaining Z_{sub} is as follows.

First, we require that the function transforming the pair θ, ε_r to $Z_{sub} = f_D(\theta, \varepsilon_r)$ must be smooth (continuous) when the amplitude and phase of (11) is increasing for a given value of M_{sub}. In other words the amplitude and phase of (11) must be a smooth function of Z_{sub} for a given value of M_{sub}. Numerical experiments, that we performed, showed that when the above relation is fulfilled each of the residua and poles resulting from consecutive applications of VF algorithm (for successive values of Z_{sub}), are smooth functions of Z_{sub}. These functions can be easily approximated. The functions can be approximated by applying the algorithms implemented in Mathematica, Mathcad etc. as well as with the usage of VF algorithm. We used the latter one by treating Z_{sub} as the time argument, applying IFFT, then VF approximation and finally retransformation to Z_{sub} domain. During calculations of (11) we used Olver expansion [6] to obtain the Hankel function with complex order and its derivative values.

In order to transform a pair of variables θ, ε_r to the variable Z_{sub} we propose to use the functions in (13).

$$f_{D1}(\theta,\varepsilon_r) = \left[\frac{\varepsilon_r^{\,b\cdot\theta^c}}{a}\right]. \quad (13)$$

Relation [X] in (13) means the biggest integer value not bigger than X. There are three extra parameters in (13). The values of *a*, *b*, *c* and *d* are derived experimentally through analysis of the results of (11a) calculations for a given values of M_{sub} in a considered range of θ and ε_r values. The main task of *b* and *c* values adjustment is to make amplitude and phase of (11) a smooth function Z_{sub} for a given value of M_{sub}. The values of *b* and *c* depend on the limits of θ and ε_r values which are taken into consideration (for which the impulse response must be obtained). The small phase function fluctuations in Z_{sub} domain can be smoothed in order to improve the performance of VF approximation. This smoothing of the phase function of (11a) does not cause meaningful error in calculations of UWB pulse distortion, what will be shown in the next section. By changing the value of parameter *a* we control the accuracy of θ x $\varepsilon_r \rightarrow Z_{sub}$ transformation. The bigger accuracy of transformation is, the more different values of (13) are. In other words if the results of (13) for a given pairs of values of θ, ε_r are the same, the values of (11a) for these pairs of θ, ε_r must be in the margin of maximum allowed relative deviation of approximation (assumed for this part of the impulse response derivation, for example 0.1% deviation from the accurate frequency domain results.). The exemplary results of the amplitude and the phase functions of (11a) with respect to Z_{sub} for a given M_{sub} value are shown in Fig. 2 and Fig. 3. We used (13) formula with *b* = 0.1 and *c* = 2 for $\theta \in <3\cdot10^{-4}, \pi>$ and $\varepsilon_r \in <45.0, 50.0>$.

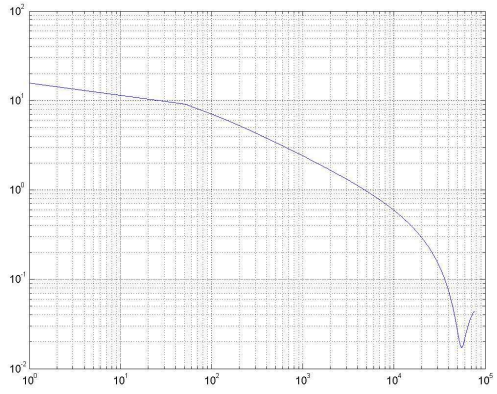

Fig. 2. Amplitude of (11a): b=0.2, c=2, $\theta\in<3\cdot10^{-4}, \pi>$ $\varepsilon_r \in<45.0, 50.0>$.

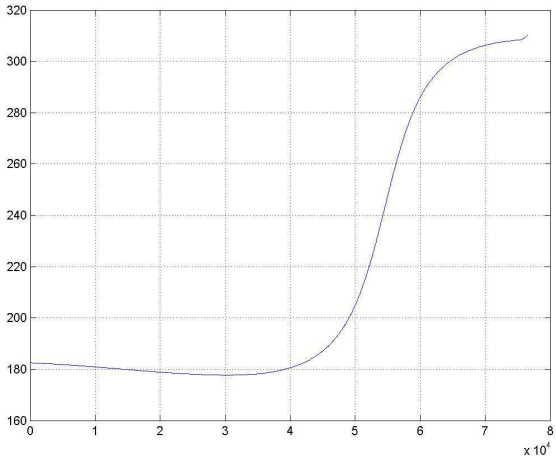

Fig. 3. Phase of (11a): b=0.2, c=2, $\theta\in<3\cdot10^{-4}, \pi>$ $\varepsilon_r \in<45.0, 50.0>$.

After experimental derivation of *a, b, c* values we obtain the time-domain equivalent of (3) in the following form:

$$H_{A2D}(\omega) \approx \sqrt{R\theta}\cdot\sum_{k=1}^{K}\frac{C_{2k}(Z_{sub})\cdot 2c/R}{j\omega + A_{2k}(Z_{sub})\cdot 2c/R} \quad (14)$$

The values of K from (14) as well as J from (9) depend on M_{sub} and X_{dsub} limits as well as the maximum allowed VF approximation relative deviation. In order to keep the relative deviation of approximation under 0.1% for the range of parameters (ω, R, θ, L_d) given in the article, K and J values should equal above 10.

Having (9) and (14), the new impulse response of a creeping ray for the case of a dielectric object is easily obtained by applying the inverse Laplace transform. The form of the impulse response components are given in (15) and (16) (poles values have negative sign)

$$h_{A1}(t) \approx \sqrt{\frac{L}{4\pi}}\cdot\sum_{j=1}^{J}\frac{C_{1j}2v}{L\theta^2}e^{\frac{A_{1j}\cdot 2v}{L\theta^2}t} \quad (15)$$

$$h_{A2D}(t) \approx \sqrt{R\theta} \cdot \sum_{k=1}^{K} \frac{C_{2k}(Z_{sub}) \cdot 2c}{R} e^{-\frac{A_{2k}(Z_{sub}) 2c}{R} t} \tag{16}$$

IV. NUMERICAL CALCULATION RESULTS

In this section we present the results of simulations of diffraction of exemplary UWB pulse on a dielectric 2D convex obstacle. We compare IFFT results incorporating accurate frequency-domain formulas [4] with the results obtained directly in the time-domain by applying the impulse response, derived with the procedure described in the previous section. The results are shown in Fig. 4-6. The delay factors were not taken into consideration in calculation of the results. The maximum value of the incident pulse is normalized to the maximum value of the distorted pulse. The time axes are scaled in ns. The incident Gauss pulse is calculated by formula (17) with t_c = 1.5ns and w = 0.7ns.

$$p(t) = \left[1 - 4\pi\left(\frac{t - t_c}{w}\right)^2\right] e^{-2\pi\left(\frac{t-t_c}{w}\right)^2} \tag{17}$$

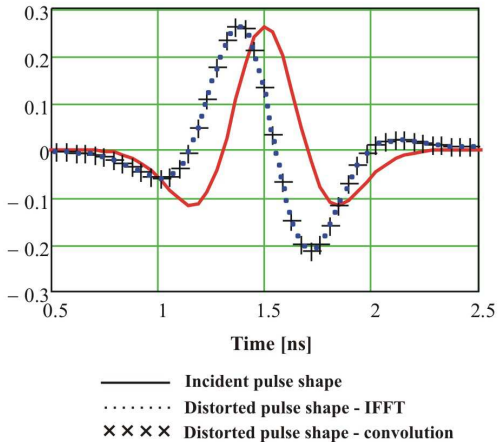

Fig. 4. Incident and distorted UWB Gauss pulse for parameters values: R = 0.25m, θ = 0.1, ε_r = 45, L=1.5.

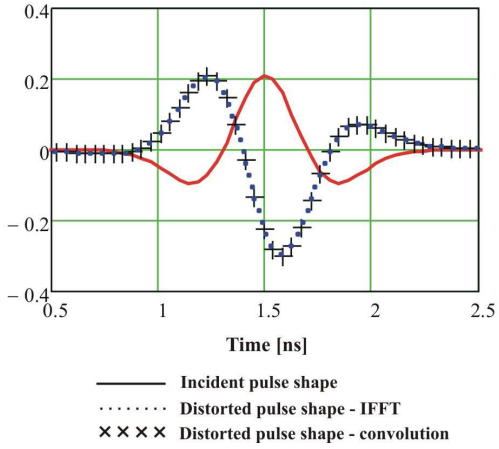

Fig. 5. Incident and distorted UWB Gauss pulse for parameters values: R = 0.25m, θ = 0.5, ε_r = 50, L=1.5.

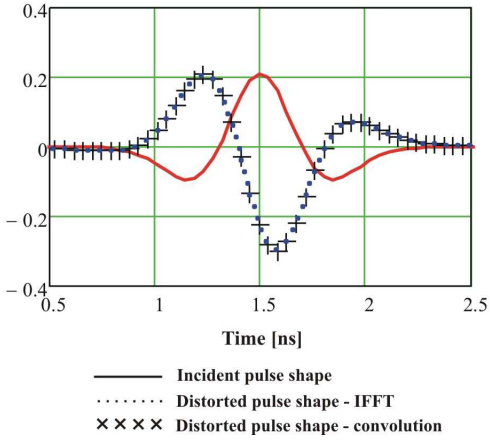

Fig. 6. Incident and distorted UWB Gauss pulse for parameters values: R = 0.35m, θ = 0.7, ε_r = 50, L=1.5.

V. CONCLUSIONS

The aim of the article was to present the new approach for derivation of an impusle response of a dielectric convex object. This object can be an effective model of a real convex obstacles, e.g. human body, that can occur in an UWB channel.

We verified the new method by performing the simulations with the usage of the impulse response derived for the given θ and ε_r limits. We showed that there is a very good agreement between convolution and IFFT (reference) results (Fig. 4-6).

The form of the impulse response is very simple, and can be effectively applied to simulations of UWB wave propagation on convex obstacles. We can apply direct analytical calculations of convolutions or use faster recursive numerical procedures of convolutions and take advantage of the fact that the components of the impulse response describe low-pass filters. Then part of the impulse response components can be ommited during calculation of a paricular ray response or can be approximated by a delayed delta Dirac function.

REFERENCES

[1] P. Górniak, W. Bandurski, "The New Vector Fitting Approach to Modeling of UWB Channels Containing Convex Obstacles", 6th European Conference on Antennas and Propagation, Prague, 26-30 March 2012.

[2] M. Ghaddar, L. Talbi, T. Denidni, A. Sebak, "A Conducting Cylinder for Modeling Human Body Presence in Indoor Proipagation Channel", IEEE Transactions on antennas and Propagation, vol. 55, no. 11, pp. 3099–3103, November 2007

[3] T. Ida, T. Ishihara, K. Goto, "Frequency-Domain and Time-Domain Novel Uniform Asymptotic Solutions for Scattered Fileds by an Impedance Cylinder and a Dielectric Cylinder", IEICE Transactions on Electronics, vol. E88-C, no. 11, pp. 2124–2135, November 2005.

[4] T. Sasamori, T.Uno, S. Adachi, "High-Frequency Analysis of Electromagnetic Scattering due to a Dielectric Cylinder" ", IEICE Transactions on Electronics, vol. J78-C-I, no. 1, pp. 9–19, January 1995.

[5] L. Pearson, "A scheme for Automatic Computation of Fock-Type Integrals", IEEE Transactions on Antennas and Propagation, vol. 35, no. 10, pp. 1111–1118, October 1987.

[6] R. Paknys, "Evaluation of Hankel Functions with Complex Argument and Complex rder", IEEE Transactions on Antennas and Propagation, vol. 40, no. 55, pp. 569–578, May 1992.